

UC Berkeley

UC Berkeley Previously Published Works

Title

Carbon fluxes and interannual drivers in a temperate forest ecosystem assessed through comparison of top-down and bottom-up approaches

Permalink

<https://escholarship.org/uc/item/1s69x9mm>

Authors

Ouimette, Andrew P

Ollinger, Scott V

Richardson, Andrew D

et al.

Publication Date

2018

DOI

10.1016/j.agrformet2018.03.017

Peer reviewed

# Carbon fluxes and interannual drivers in a temperate forest ecosystem assessed through comparison of top-down and bottom-up approaches

Andrew P. Ouimette<sup>a,\*</sup>, Scott V. Ollinger<sup>a</sup>, Andrew D. Richardson<sup>b</sup>, David Y. Hollinger<sup>c</sup>, Trevor F. Keenan<sup>d,e</sup>, Lucie C. Lepine<sup>a</sup>, Matthew A. Vadeboncoeur<sup>a</sup>

<sup>a</sup>University of New Hampshire, Earth Systems Research Center, Durham, NH 03824, USA <sup>b</sup>Harvard University, Department of Organismic and Evolutionary Biology, Cambridge MA 02138, USA <sup>c</sup>USDA Forest Service, Northern Research Station, 271 Mast Rd, Durham, NH 03824, USA <sup>d</sup>Earth Sciences Division, Lawrence Berkeley National Lab, Berkeley, CA 94709, USA <sup>e</sup>Department of Environmental Science, Policy and Management, UC Berkeley, Berkeley, CA 94709, USA

\* Corresponding author. E-mail address: Andrew.Ouimette@unh.edu (A.P. Ouimette).

## Abstract

Despite decades of research, gaining a comprehensive understanding of carbon (C) cycling in forests remains a considerable challenge. Uncertainties stem from persistent methodological limitations and the difficulty of resolving top-down estimates of ecosystem C exchange with bottom-up measurements of individual pools and fluxes. To address this, we derived estimates and associated uncertainties of ecosystem C fluxes for a 100–125 year old mixed temperate forest stand at the Bartlett Experimental Forest, New Hampshire, USA, using three different approaches: (1) tower-based eddy covariance, (2) a biometric approach involving C flux measurements of individual ecosystem subcomponents, and (3) an inventory approach involving changes in major C stocks over time. Our analysis made use of 13 years of data, collected over the period from 2004 to 2016. Estimates of mean annual net ecosystem production (NEP) ranged from 120 to 133gCm<sup>-2</sup>, demonstrating strong agreement among methods and suggesting that this aging forest acts as a moderate C sink. The use of multiple approaches to measure C fluxes and their uncertainties helped place constraints on difficult-to-measure processes such as aboveground contributions to ecosystem respiration and belowground allocation to mycorrhizal fungal biomass (which was estimated at 20% of net primary production). Analysis of interannual variability in C fluxes revealed a decoupling between annual wood growth and either current year or lagged NEP or GPP, suggesting that source limitation (C supply) is likely not controlling rates of wood production, at least on an interannual scale. Results also demonstrated a strong association between the maximum rate of C uptake during the growing season ( $A_{max}$ ) and the length of the vernal window, defined as the period of time between soil thaw and the onset of photosynthesis. This suggests an important, but poorly understood, influence of winter and spring climate on mid-summer canopy physiology. Efforts to

resolve the mechanisms responsible should be prioritized in light of ongoing and predicted changes in climate for the northeastern U.S. region, particularly during the winter and winter-spring transition period.

Keywords: Eddy covariance, Biometric, Carbon fluxes, Vernal window, Mycorrhizae

## 1. Introduction

Forests represent the dominant land cover type in the northeastern United States (Foster and Aber, 2004) and are widely regarded as carbon sinks given their state of recovery from widespread agriculture in the 19th century (Caspersen et al., 2000; Goodale et al., 2002). However, the ability of these aging secondary forests to continue to act as net carbon sinks as they transition to late-successional stands is unclear. Although a commonly accepted view is that old-growth forests are carbon neutral (Odum, 1969), more recent reviews indicate that late successional forests can often act as net carbon sinks (Luyssaert et al., 2008). Additional data on the net carbon flux of eastern North American forests should improve our understanding of the ability of these forests to continue to act as net carbon sinks.

Approaches to estimating net C exchange in forests include eddy covariance flux towers, biometric estimates of growth and respiration, and changes in important C stocks over time. Each of these has inherent strengths and limitations. Eddy flux towers provide direct measurements of net CO<sub>2</sub> exchange at high temporal resolution, but can suffer from unquantified advective losses (e.g. Aubinet et al., 2012; Novick et al., 2014; van Gorsel et al., 2009; Vickers et al., 2012), data gaps during calm periods, and non-CO<sub>2</sub> C fluxes. Eddy flux measurements also lack information on how C is allocated to various ecosystem components (e.g. foliage, wood, fine roots, mycorrhizal fungi), that possess a range of functions and C residence times and that are required to more fully test ecosystem models.

Biometric approaches that quantify the difference between net primary production (NPP) and heterotrophic respiration ( $R_h$ ), can provide independent estimates of net ecosystem C exchange and can shed light on how C is allocated among various pools. However, this requires estimates of difficult-to-measure fluxes (e.g. belowground biomass production), which can introduce substantial uncertainties (Clark et al., 2001).

Estimating net C exchange from changes in major C stocks offer yet another approach, the benefits of which include its straightforward nature and lack of reliance on difficult-to-measure fluxes. However, belowground C pools are large and notoriously variable, making change detection extremely difficult (Vadeboncoeur et al., 2012). And, on its own, this method doesn't offer insight into mechanisms or subcomponent C fluxes. Consistency between top-down and bottom-up C quantification approaches can greatly enhance confidence in estimates of an ecosystem's C balance. Taken together, data from multiple approaches can also provide estimates on a full suite of

ecosystem C fluxes to which ecosystem models can be more thoroughly compared.

Here we used multiple methodological approaches to compile a comprehensive carbon budget for an aging (100–125 year old) mixed temperate forest in New England (Bartlett Experimental Forest, NH). This included a comparison of net and gross ecosystem C fluxes using 3 complementary approaches (eddy covariance, biometric estimates of NPP and  $R_h$ , and a modified C inventory approach) for 13 years (2004–2016) of data. We included estimates of uncertainty for all three approaches, and highlight how the comparison of several independent methodological approaches provided more confidence in estimates of difficult-to-measure respiratory and belowground fluxes. Finally, drivers of interannual variations of C fluxes were evaluated by comparing net ecosystem production (NEP), gross primary production (GPP), ecosystem respiration ( $R_e$ ), and wood growth to an array of climatic, phenological, and biological variables.

## 2. Methods

### 2.1. Site description

Bartlett Experimental Forest (BEF) (44°06'N, 71°3'W) is located within the White Mountain National Forest in north-central New Hampshire, USA (Fig. 1). The climate is humid continental with cool summers (mean July temperature, 19°C) and cold winters (mean January temperature, –9°C). Mean annual temperature is 6°C and mean annual precipitation is 1270mm (for additional site information, see <http://www.fs.fed.us/ne/durham/4155/bartlett.htm>). The forest within the eddy covariance tower footprint was cutover circa 1900 and some areas were damaged by the 1938 hurricane. In the past decade there has also been small-scale forest management just outside the tower footprint, but mean stand age is roughly 100–125 years. Average canopy height is approximately 20–22m within the tower footprint and is composed of a diverse assemblage of species including *Acer rubrum* (29%), *Fagus grandifolia* (25%), *Tsuga canadensis* (14%), *Betula alleghaniensis* (9%), *Betula papyrifera* (6%), *Fraxinus americana* (5%), *Acer saccharum* (5%), and *Populus grandidentata* (4%), with minor amounts of other coniferous species. Soils are generally acidic Spodosols and Inceptisols derived from granitic till, and poor in both Ca and P (Vadeboncoeur et al., 2014). Foliar N and ecosystem N cycling rates are both low relative to other mixed hardwood sites in the region (Ollinger et al., 2002).

In 2003, BEF was adopted as a NASA North American Carbon Program (NACP) Tier-2 field research and validation site. During this time a 26.5m tower was installed in a low-elevation (290m) mixed hardwood stand for the purpose of making eddy covariance measurements of the forest–atmosphere exchange of carbon dioxide, water, and sensible heat. Continuous flux and meteorological measurements began in January 2004 and are ongoing (data are available online from AmeriFlux, <http://www.public.ornl.gov/ameriflux/>).

In 2004, 12 FIA-style plots (Hollinger, 2008) were established across a 1km by 1km area centered on the flux tower for the purpose of making complimentary biometric measurements of carbon pools and fluxes. BEF is also a NEON relocatable site (construction began in the summer of 2013) and the new flux tower is located within 100m of the existing flux tower.

## 2.2. Eddy covariance estimates of C flux and uncertainty

The eddy covariance system provides direct measurements of the net ecosystem exchange rate of CO<sub>2</sub> between the forest canopy and the atmosphere (NEE). Eddy covariance estimates of NEE, after accounting for a change in sign, are equivalent to net ecosystem production (NEPEC) assuming that sources and sinks of inorganic C are negligible (Chapin et al., 2006).

Forest-atmosphere CO<sub>2</sub> flux (NEE) was measured at a height of 25m with an eddy covariance system consisting of a model SAT-211/ 3K 3-axis sonic anemometer (Applied Technologies, Longmont, Colo.) and ducted to a model LI-6262 CO<sub>2</sub>/H<sub>2</sub>O infrared gas analyzer (Li-Cor, Lincoln, Neb.), through 2500cm of 0.476cm ID polyethylene tubing at 75ccs<sup>-1</sup> with data recorded at 5 Hz and fluxes (covariances) calculated every 30 min. In 2014 the LI-6262 was replaced with a model LI-7200 analyzer. Average (30min) meteorological variables (e.g. air and soil temperatures, incoming solar radiation, etc.) measured at the tower were recorded concurrently. The instrument configuration, calibration protocol, QA/QC, and data processing procedures were identical to those used at the Howland AmeriFlux site in central Maine, USA, and have been documented in detail elsewhere (Hollinger et al., 2004). Site visits by the AmeriFlux Tech Team took place in the summers 2006 and 2016, to confirm overall quality of the flux and meteorological measurements.

Half-hourly NEE data were filtered to remove time periods with low atmospheric turbulence where advective losses were likely significant similar to Barr et al. (2013). Following this approach a median ustar threshold of  $0.50 \pm 0.10$  was detected and used across all seasons and years. Gaps in NEE were filled using the (Barr et al., 2004) FluxnetCanada method (FCM) with slight modifications, including: mild exclusion of NEE outliers; use of a weighted mean of soil and air temperature as the independent variable for estimating Re; and delineation of nighttime periods from global shortwave radiation of less than 5W m<sup>2</sup>. Random uncertainties in NEE were estimated following (Richardson and Hollinger, 2007). NEE was partitioned into gross primary production (GPP<sub>EC</sub>) and total ecosystem respiration (Re<sub>EC</sub>) using the FCM method. Further details of the gap-filling and partitioning methods used are presented in Barr et al. (2013).

## 2.3. Biometric estimates of carbon fluxes with uncertainty

In addition to eddy covariance, we used measurements of individual ecosystem components to make biometric estimates of gross and net carbon

fluxes. For biometric estimates of NEP, ( $NEP_B$ ), we subtracted heterotrophic respiration ( $R_h$ ), including respiration from dead woody biomass ( $R_{DW}$ ), and the heterotrophic portion of soil respiration ( $R_{SH}$ ), from total net primary production (NPP), including NPP from foliage, aboveground woody tissues, understory production, fine and coarse roots, and mycorrhizae (Table 1). We also calculated biometric estimates of gross primary production ( $GPP_B$ ) and ecosystem respiration ( $Re_B$ ).  $GPP_B$  was calculated by summing all sources of NPP, with all sources of autotrophic respiration, including autotrophic respiration from foliage, aboveground wood, and the autotrophic portion of soil respiration (Table 1). Biometric estimates of  $Re_B$  were calculated by summing all sources of heterotrophic and autotrophic respiration including total soil respiration, respiration from coarse woody debris and standing dead wood, as well as from foliar and woody tissues.

### 2.3.1. Aboveground production

Beginning in 2004 estimates of aboveground carbon pools and fluxes were made on 12 plots within a 1km by 1km area centered on the flux tower with a similar layout, but larger size, to that described in Hollinger (2008). Each of the 12 plots contains four 10m radius subplots for a total of 48 subplots within the 1 km<sup>2</sup> footprint of the flux tower. Each subplot contains 3 soil respiration collars, 2 litterfall traps, and 1 branchfall collection tarp, resulting in 154 soil respiration collars, 96 litterfall traps, and 48 branchfall collection tarps within the 1 km<sup>2</sup> footprint around the flux tower. We followed established methods for estimating woody biomass and production (Clark et al., 2001; Curtis, 2008), litterfall and branchfall (Bernier et al., 2008), and biomass of coarse woody debris (Valentine et al., 2008).

In each of the 48 subplots within the 1 km<sup>2</sup> footprint of the flux tower the location, diameter at breast height (dbh), and species of all trees greater than 12.7cm were recorded annually from 2004 to 2016. For small trees (2.54 to 12.7 cm dbh), all trees were measured within a 2m radius microplot within each subplot, with microplot center 4 m (at an azimuth of 90°) from subplot center. Dbh measurements on all trees were made each year after leaf fall in late October/early November by the same three person team using paint markings to improve the consistency of repeat measurements.

To calculate the NPP of live woody tissues (both large and small trees), estimates of live woody biomass of the previous year were subtracted from current year estimates, while holding the dbh of any trees that died throughout the study period constant at the last live measurement as recommended in Clark et al. (2001). Above and belowground woody NPP and associated uncertainty were then calculated using a Monte Carlo simulation approach similar to that described by Yanai et al. (2010). This approach estimates the statistical distribution of the output of a calculation through multiple iterations in which the input data are chosen randomly based on their underlying distributions. Specifically for each iteration the measured diameter of each tree was allowed to vary randomly with a normal

distribution using standard deviation (s.d.) of 0.1cm. The percent carbon (%C) of woody material was varied randomly for both hardwood species (mean of 48% and s.d. of 1%) and for coniferous species (mean of 50% and s.d. of 1%). Because many allometric equations lack estimates of error, we simulated uncertainty due to allometric modeling by randomly selecting between 3 different sets of allometric models. Two local species specific allometric models (Whittaker et al., 1974; Young et al., 1980), and one set of generalized (taxonomically grouped) allometric models (Chojnacky et al., 2014) were chosen randomly for each iteration. For each iteration, %C and choice of allometric model were held constant for all years. The mean and 95% confidence interval of 1000 iterations were used to derive NPP (difference between current and previous year woody biomass), and associated uncertainty measurements for each subplot for each year. Uncertainties from the Monte Carlo simulations were propagated with spatial (plot to plot) and temporal variability using classical error propagation techniques (see Section 2.6.).

Annual branchfall collections were used to calculate a mean estimate of the contribution of branchfall to woody carbon flux, while annual foliar and fruit/flower collections were used to calculate a mean estimate of carbon flux to foliar/fruit/flower production. Branchfall (<5 cm diameter) was collected once per year in October, using one 3.34 m<sup>2</sup> branchfall tarp on each subplot for a total of 48 branchfall tarps. Annual foliar and fruit/flower production were estimated by collection of aboveground litterfall using 2 litterfall traps (0.24 m<sup>2</sup>) randomly placed in each subplot. Litter was collected 2-5 times each fall and once the following spring. To convert branchfall and litterfall into C fluxes, annual biomass collections were multiplied by the mean %C (49%). Uncertainty due to %C, spatial variability, and temporal variability were summed using standard error propagation techniques (using a 2% standard error for %C) and reported as 95% confidence intervals.

The contribution of understory production to total NPP was estimated using allometric models and annual seedling surveys on 2m diameter microplots in each of the 48 subplots, following methods described in (Chojnacky and Milton, 2008). Uncertainty due to spatial and temporal variation as well as uncertainties in %C were propagated using standard techniques.

### 2.3.2. Belowground production

Production of fine roots (<2 mm diameter) was estimated using ingrowth cores. Within the tower footprint, 90 individual year-long (late October 2013-late October 2014) cores were installed to 30 cm depth. Total root mass per area found in the ingrowth cores was assumed to represent annual fine root production. Estimates were not corrected for the tendency of cores to overestimate root biomass or to account for root growth below 30 cm depth. Omitting these two biases likely has a small effect on estimates of root production; Park et al. (2007) found that in stands at Bartlett Experimental Forest cores tended to overestimate by 27% (compared to soil pits) while

sampling to only 30cm led to a 28% underestimate of root biomass. Uncertainty due to spatial variation and %C ( $49\% \pm 2\%$ ), were propagated using standard error propagation techniques.

Estimates of ectomycorrhizal (ECM) fungal production were made using a stable isotope approach described in (Hobbie and Hobbie, 2008; Ouimette et al., 2013). Briefly, ECM fungi discriminate against  $^{15}\text{N}$  during the creation of nitrogen (N) transfer compounds for plant hosts. The fraction of nitrogen transferred to ECM hosts ( $\text{Tr}$ ) can be calculated (Eq. (1)), using the fractionation factor during mycorrhizal transfer of N ( $\Delta f$ ), and the  $^{15}\text{N}:^{14}\text{N}$  ratios (expressed as  $\delta^{15}\text{N}$ ) in plant ( $\delta^{15}\text{N}_{\text{Plant}}$ ) and soil available N ( $\delta^{15}\text{N}_{\text{Avail}}$ ).

$$\text{Tr} = 1 + (\delta^{15}\text{N}_{\text{Plant}} - \delta^{15}\text{N}_{\text{Avail}}) / \Delta f \quad (1)$$

The amount of C allocated to ECM fungal biomass can then be calculated stoichiometrically (Eq. (2)) using the fraction of N transferred to plant host ( $\text{Tr}$ ), plant host N demand, and the C:N ratio of fungi as:

$$\text{NPP}_{\text{fungi}} = (1/\text{Tr} - 1) \times \text{N}_{\text{demand}} \times \text{C}/\text{N}_{\text{fungi}} \times f_{\text{ECM}} \quad (2)$$

where  $\text{N}_{\text{demand}}$  is annual plant N demand,  $\text{C}/\text{N}_{\text{fungi}}$  is the C/N ratio of ECM fungi, and  $f_{\text{ECM}}$  is the biomass fraction of ECM trees within the stand. Here we used the  $\delta^{15}\text{N}$  of co-located (by depth) root and soil samples to calculate  $\text{Tr}$ , and net annual changes in foliar, wood, and fine root N stocks to calculate plant N demand.

As an alternative approach to assess our estimates of mycorrhizal production we compared biometric estimates of NEP to estimates of NEP from eddy covariance and C inventory approaches. Specifically, production of mycorrhizal fungi was initially included as a component of  $\text{NEP}_B$  ( $\text{NEP}_B$  was calculated as total NPP minus the heterotrophic portion of ecosystem respiration - Table 1). We additionally calculated  $\text{NEP}_B$  omitting our measured mycorrhizal fungal C flux. To do this we ran Monte Carlo simulations (10,000 iterations) to calculate  $\text{NEP}_B$ , allowing estimates of each component of NPP and  $R_h$  to vary with their measured/estimated distributions (similar to Yanai et al., 2010). Estimates of  $\text{NEP}_B$  that both included and omitted our estimate of mycorrhizal NPP were compared to NEP estimates from eddy covariance and C inventory approaches.

Additionally, we estimated total belowground carbon allocation (TBCA) using the mass balance approach described in Raich and Nadelhoffer (1989) and Davidson et al. (2002). Specifically, TBCA was estimated as the difference between total soil respiration and fine litterfall. This approach assumes that changes in the stocks of soil organic matter, roots, and litter are in near steady state or small relative to soil respiration and litterfall.

### 2.3.3. Soil respiration

Soil respiration was measured using infra-red gas analyzers (IRGA) in conjunction with both static chambers and autochambers. The static



chambers consisted of a 10inch PVC collar permanently inserted ~5 cm into the soil. Three collars per subplot (144 chambers across the 1 km<sup>2</sup> tower footprint) were measured roughly every 3 weeks during the snow-free portion of each year using a LICOR 820 CO<sub>2</sub> gas analyzer during 2004–2007 (>3400 measurements). Simultaneous soil moisture and temperature measurements were made at 5cm soil depth. Chamber volumes were measured every year but were approximately 5.5l. After scrubbing the chamber to ~30 ppm below ambient CO<sub>2</sub> concentrations, concentrations were measured every 2s over a 60s period. The flux was calculated as follows: flux(umoles CO<sub>2</sub> m<sup>-2</sup>sec<sup>-1</sup>) = PV/RTA \* (dxCO<sub>2</sub>/dt), where P is chamber pressure in bar, V is chamber volume in m<sup>3</sup>, T is chamber air temperature in Kelvin, A is chamber area in m<sup>2</sup>, R is the ideal gas law constant or 0.0000834472 m<sup>3</sup>barK<sup>-1</sup>mole<sup>-1</sup>, and (dxCO<sub>2</sub>/dt) is the rate of change of the mole fraction CO<sub>2</sub> concentration in the chamber (umoles sec<sup>-1</sup>).

During 2007–2008 five autochambers were operated on a single plot continuously during the snow-free periods of the year (>5600 measurements) following methods described in (Phillips et al., 2010).

To derive annual soil CO<sub>2</sub> flux estimates for both static and autochambers, measured CO<sub>2</sub> flux rates from the chambers were fit using a Gauss-Newton optimization method in JMP 13.0 statistical software (SAS 2016), to a suite of respiration models (Richardson et al., 2006) including Q<sub>10</sub> temperature, temperature and time varying Q<sub>10</sub>, soil water content modulated Q<sub>10</sub>, Arrhenius, and logistic response functions. For most models, fit parameters did not vary significantly between years for either static or autochambers (results not shown), thus measurements from all years were pooled to derive modeled parameters for each chamber type.

Model best fits (using data from 2004 to 2008) were applied to continuous (every 30min) temperature and moisture measurements made at the base of the eddy covariance flux tower (5cm depth) to estimate annual soil CO<sub>2</sub> flux rates for each chamber type during all years (2004–2016). Lower and upper 95% confidence intervals were estimated for each model and chamber type. Since annual CO<sub>2</sub> flux rates and model goodness of fit varied minimally among model types, results from a logistic fit are reported to minimize gap-filling artifacts between chamber-based soil respiration and eddy covariance towerbased ecosystem respiration estimates (also modeled logistically).

Soil CO<sub>2</sub> flux during winter months was estimated using the logistic fit (above), derived from measurements during the snow-free season. Because winter respiration fluxes can be similar in magnitude to NEP, a more direct estimate of wintertime respiration was also made during the winter of 2011–2012 using the soda lime technique described in Grogan (1998) and Keith and Wong (2006). Briefly, roughly 800g of oven-dried, soda lime were left from November 17, 2011 to March 21, 2012 (125 days), in an enclosed chamber (surface area=0.06783m<sup>2</sup>). All post-collection soda lime weights were blank-corrected using the mean of 6 field blanks prior to flux

calculation. Because estimates of winter respiration using the soda lime technique (data not shown) were similar to those estimated using a logistic fit from chamber measurements, soil CO<sub>2</sub> flux during winter months was estimated using the logistic temperature response model described above.

To scale up to the forest stand, chamber-based soil CO<sub>2</sub> flux measurements were corrected for the area occupied by rocks and tree root crowns (roughly 13%) similar to Bae et al. (2015). Uncertainty was estimated by propagating uncertainty due to soil rockiness, model fit, as well as spatial and temporal variability.

#### 2.3.4. Partitioning R<sub>s</sub> into autotrophic and heterotrophic components

No attempt was made to directly measure the contribution of autotrophic (R<sub>SA</sub>) or heterotrophic (R<sub>SH</sub>) respiration to total soil respiration (R<sub>S</sub>). Instead we used several different approaches to partition R<sub>S</sub>. First, the Global Database of Soil Respiration Version 3 (Bond-Lamberty and Thomson, 2014) was used to derive a relationship between R<sub>SH</sub> and R<sub>S</sub>. We used data from non-experimentally manipulated, temperate, deciduous, forest ecosystems with quality check flags of Q0, Q01, Q02, and Q03 (n=114) to derive the following relationship between annual R<sub>SH</sub> and R<sub>S</sub>:  $R_{SH} = 1.925 (\pm 34.392) + R_S * 0.534 (\pm 0.045)$ . This relationship was used with measured estimates of mean annual R<sub>S</sub> to derive annual estimates of R<sub>SH</sub> (and R<sub>SA</sub> by difference). Monte Carlo simulations using the uncertainty in annual R<sub>S</sub> and in the relationship between R<sub>S</sub> and R<sub>SH</sub> were used to estimate uncertainty in R<sub>SH</sub> and R<sub>SA</sub> and reported as 95% confidence intervals as described above. As an additional approach to help assess the uncertainty in estimates of R<sub>SH</sub>, we estimated R<sub>SH</sub> independently by summing all detritus inputs (branchfall, foliar litterfall and root and mycorrhizal production) following (Bond-Lamberty et al., 2004). This independent approach was compared to estimates of R<sub>SH</sub> using the partitioning method described above.

#### 2.3.5. Respiration from woody biomass

To estimate annual respiratory losses from dead woody material, estimates of dead woody C stocks were multiplied by the mean decay rate for hardwood species from Russell et al. (2014) (hardwood species comprised 97% of the standing dead woody biomass pool). Dead woody biomass was assumed to have 49% C (Thomas and Martin, 2012) with a standard error of 2%. Uncertainty due to initial estimates of dead woody biomass, %C, and decay rates from Russell et al. (2014) were propagated using standard error propagation techniques and reported as 95% confidence intervals.

No direct measurements of respiration from live woody biomass were made. Instead, we used two approaches to estimate losses of CO<sub>2</sub> from live woody biomass. First, to derive a “biometric” estimate that was independent of eddy covariance measurements, live woody respiration was assumed to be equal to 0.118 of biometric GPP, the median ratio of woody respiration to

GPP of mature and old growth forests (>50years old; n=16) reported in the database of (Litton et al., 2007). Uncertainty was reported as 0.75 of the mean annual flux.

Additionally, we derived estimates of aboveground respiration (including foliage and live and dead woody biomass) as the annual difference between eddy covariance estimates of ecosystem respiration and soil respiration from chamber measurements.

### 2.3.6. Foliar respiration

Dark respiration for live foliage was estimated using species-specific leaf-level measurements of dark respiration and scaled to the stand and annual scales using estimates of stand leaf area index (LAI) and a temperature sensitive  $Q_{10}$  response function. Specifically, gas exchange measurements of dark respiration were conducted during August of 2014 and July/August of 2016 on cloud-free days between 1000–1500 EST using a portable gas exchange system (LICOR-6400xt, LICOR, Lincoln, NE, USA), equipped with a standard 2×3cm leaf cuvette and a LICOR-6400-02B LED light source. During measurements  $[CO_2]$  was maintained at a value of 400ppm, relative humidity at 50%, and temperature held constant at a temperature of 24.5°C (reference temperature). Species-specific estimates of foliar dark respiration (n=75 across all species) were then weighted by the fractional contribution of each species to stand LAI to derive a stand-level dark respiration rate at the reference temperature ( $R_{dref}$ ).

A  $Q_{10}$  response function (Eq. (3)) was used to estimate dark respiration rates at temperatures other than the reference temperature using  $R_{dref}$  and half hourly measurements of air temperature (periods when PAR < 5  $\mu\text{moles m}^{-2}\text{sec}^{-1}$ ), where for Eq. (3),  $T_{air}$  and  $T_{ref}$ , were the measured air temperature and reference air temperature (24.5°C), respectively.

$$\text{Foliar dark respiration rate} = R_{dref} \times Q_{10}^{(T_{air} - T_{ref})} \quad (3)$$

Because the  $Q_{10}$  temperature response function of foliar dark respiration is known to vary over short timescales with changes in ambient temperature,  $Q_{10}$  was allowed to vary with ambient temperature following (Tjoelker et al., 2001;  $Q_{10} = 3.22 - 0.046 * \text{air temperature}$ ). Annual stand-level foliar dark respiration rates were then made by multiplying temperature adjusted dark respiration rates by estimates of stand LAI summing half hourly estimates.

Uncertainty due to variation in leaf-level dark respiration rates, as well as uncertainty in estimates LAI and the temperature response function reported in (Tjoelker et al., 2001) were quantified using Monte Carlo simulations as described above where estimates of each parameter were allow vary with their measured distributions.

### 2.4. Changes in carbon stocks ( $\Delta C$ )

To complement eddy covariance and biometric estimates of NEP, we estimated the mean annual change in total ecosystem carbon stocks ( $\Delta C$ ) using a modified carbon inventory approach. Inventory approaches rely on knowing the carbon stock of various ecosystem pools at two points in time. In closed-canopy forest stands, the pools of primary importance are live and dead woody biomass, as well as soil carbon. Here we focus on changes in woody carbon stocks and assume that changes in soil carbon stocks were minimal as was found from measurements at mature stands in nearby Hubbard Brook Experimental Forest (Yanai et al., 2013). Changes in soil carbon stocks would be very difficult to detect over a 13-year study period (Vadeboncoeur et al., 2012). Instead, in these mature (100–125-year old) stands we assumed that there was little to no net change in annual soil C stocks; however, we included an uncertainty of  $\pm 40 \text{ g C m}^{-2} \text{ yr}^{-1}$  (Post and Kwon, 2000).

To estimate changes in woody carbon stocks, we used a modified inventory approach. First, in 2004, we made initial measurements of standing live and dead woody biomass using the allometric approach described above (Section 2.3.1), except that standing dead woody biomass was adjusted using species- and decay-class specific density reduction factors from Harmon et al. (2011), and structural loss adjustment factors from Domke et al. (2011). In 2004 we also made estimates of dead woody biomass in coarse woody debris (CWD) using field surveys. For all downed woody material  $> 7.6 \text{ cm}$ , estimates of CWD decay class and volume were estimated using 3 methods: line intersect sampling (LIS), modified transect relascope sampling (MTRS), and fixed plot sampling, see Pesonen et al. (2009) and Valentine et al. (2008) for details of each method type. For the present study, two 100m transects (LIS), one 1m transect (MTRS), or four 1 m<sup>2</sup> subplots per each of the 12 FIA style plots were sampled. CWD volume was then multiplied by species- and decay class- specific density values from Harmon et al. (2008) to estimate CWD biomass. Total dead woody biomass in 2004 was estimated as the sum of CWD and standing dead pools.

Because we had only a single measurement of standing dead biomass and CWD in 2004, we estimated changes in dead woody biomass using annual inputs to the dead woody pool (from known live tree death and measured branchfall), while accounting for loss of carbon through decay from standing and downed dead wood using a decay rate of 0.0467 (the weighted average of the rates reported in Russell et al. (2014) for hardwoods and conifers based on the proportion of standing dead wood in our plots). To derive the mean annual change in total ecosystem carbon stocks ( $\Delta C$ ) we assumed the predominantly angiosperm woody biomass was comprised of 49% C with a standard error of 2% (Thomas and Martin, 2012). Uncertainty due to initial estimates of dead woody biomass, %C, and decay rates from Russell et al. (2014), and the assumption of no changes in soil C stocks were propagated using standard error propagation techniques and reported as 95% confidence intervals.

## 2.5. Potential drivers of interannual variability

To investigate the potential drivers of interannual variation in woody NPP, NEE, GPP, and Re, we used a suite of meteorological and phenological parameters measured at the flux tower including incoming total, direct, and diffuse photosynthetically active radiation (PAR), air and soil temperature, soil thaw day, precipitation, relative humidity, vapor pressure deficit, soil moisture content, the length, start and end dates of periods of gross and net carbon uptake, as well as the length of the vernal window - defined here as the number of days between soil thaw and the onset of gross carbon uptake (where mean daily  $GPP_{EC}$  averaged over a 7 day period, exceeded  $4 \text{ umoles CO}_2 \text{ m}^{-2}\text{sec}^{-1}$ ). We also calculated a drought index by counting the number of growing season days where the volumetric water content (VWC) was less than 17.5%; a value that represented 50% of the growing season mean during 2004–2016. In addition to these meteorological and phenological parameters we collected data on biochemical and biological parameters including annual concentrations of foliar nitrogen (estimated following Smith et al. (2008)) and masting years from Potter et al. (2015). Annual estimates of growing season canopy level  $A_{max}$  and dark respiration ( $R_d$ ) from the eddy flux data were estimated using a light response curve (Eq. (4)). For this analysis, all high-quality (ustar-filtered, non-gapfilled) measurements of half hourly NEP during June–August were used with measured PAR to estimate model parameters (e.g.  $A_{max}$ ,  $R_d$ ).

$$NEP = \frac{a * PAR}{\left( \left( 1 - \frac{PAR}{2000} \right) + \frac{a * PAR}{A_{max}} \right)} - R_d \quad (4)$$

where PAR was the measured incoming photosynthetically active radiation and  $a$  was the quantum yield.

Both current year and 1year lagged annual and seasonal data from these metrics were compared to measured C fluxes using stepwise linear multiple regression analysis with AIC (Akaike information criterion) to identify significant relationships.

## 2.6. Statistical methods and uncertainty propagation

To combine estimates of uncertainty from various sources (e.g. temporal, spatial, analytical, etc.) standard uncertainty propagation techniques were used. Specifically, to add sources of uncertainty the following approach was taken:

$$SE_{(x+y)} = \sqrt{(SE_x)^2 + (SE_y)^2} \quad (5)$$

Where SE is standard error of component  $x$ ,  $y$ , or  $(x+y)$ . 95% confidence intervals were then estimated as  $1.96 * SE$ .

## 3. Results

### 3.1. Estimated carbon fluxes using multiple approaches

#### 3.1.1. Multiyear mean fluxes

Estimates and associated uncertainties of mean ecosystem C fluxes during 2004–2016 are shown in Table 1 and include components of NPP, respiratory fluxes, and estimates of NEP, GPP, and Re. Mean (2004–2016) estimates of NEPEC, NEPB, and  $\Delta C$  ranged from 120 to 133  $\text{g Cm}^{-2}\text{yr}^{-1}$ , indicating surprising consistency in multiyear mean estimates of ecosystem net carbon flux across top-down and bottom-up approaches. All three approaches indicate that this aging 100–125-year old stand is a moderate carbon sink. Eddy covariance and biometric estimates of mean (2004–2016) GPP and Re also differed by less than 5% and were statistically indistinguishable. Total belowground carbon allocation (calculated as soil respiration minus fine litterfall) was estimated at  $656 \pm 54 \text{ g Cm}^{-2}\text{yr}^{-1}$ , within the range reported for stands of similar age within BEF ( $620\text{--}681 \text{ g Cm}^{-2} \text{ yr}^{-1}$ ) (Bae et al., 2015).

The magnitude of uncertainty in NEP, GPP, and Re differed across approaches. For estimates of NEP, eddy covariance ( $132 \pm 49 \text{ g Cm}^{-2}\text{yr}^{-1}$ ) and inventory ( $133 \pm 34 \text{ g Cm}^{-2}\text{yr}^{-1}$ ) approaches had much lower uncertainty than biometric estimates of NEP ( $120 \pm 156 \text{ g Cm}^{-2}\text{yr}^{-1}$ ). Uncertainty in eddy covariance estimates originate both from the measurements themselves as well as filtering and gapfilling procedures. Estimates of the uncertainty due to potential biases in the selection of a ustar filter were not included and would increase the reported uncertainty (Fig. 2). Uncertainty in biometric estimates of NEP are largely driven by uncertainties in fine root and mycorrhizal NPP as well as the heterotrophic portion of soil respiration (17%, 36%, and 42% of total error respectively).

Because estimates of the production of mycorrhizal fungi are lacking from many forest C budget efforts, we also used Monte Carlo simulations to calculate  $\text{NEP}_B$  excluding our mycorrhizal C flux estimates, using only mean fluxes and uncertainty from the other components of  $\text{NEP}_B$ . Excluding our estimates of mycorrhizal production resulted in  $\text{NEP}_B$  near zero ( $-3 \pm 123 \text{ g Cm}^{-2}\text{yr}^{-1}$ ), and an inconsistency between  $\text{NEP}_B$  and both  $\text{NEP}_{EC}$  and  $\Delta C$ .

#### 3.1.2. Components of NPP

Mean annual NPP was estimated at  $615 \pm 118 \text{ g Cm}^{-2}\text{yr}^{-1}$ . Growth of woody biomass including aboveground components of large and small trees, and replacement of branchfall comprised approximately 33% of total NPP ( $238 \pm 30 \text{ g Cm}^{-2}\text{yr}^{-1}$ ). Annual production of foliage, fruits, flowers, and seedlings was estimated at  $143 \pm 15 \text{ g Cm}^{-2}\text{yr}^{-1}$  or 23% of total NPP. This value may be an underestimate due to removal of seeds from litter baskets by small mammals. Estimates of fine root production and production of mycorrhizae were  $110 \pm 64$  and  $124 \pm 93 \text{ g Cm}^{-2}\text{yr}^{-1}$ , respectively, and, along with coarse woody roots, resulted in a belowground production estimate that was 44% of total NPP. Uncertainties in estimated belowground C fluxes to mycorrhizae are unknown, but are likely to be large. If we set this value at

75% of our measured estimate, then uncertainties in belowground fluxes (including fine root production) accounted for 94% of the uncertainty in total NPP.

### 3.1.3. Respiratory fluxes

Estimates of autotrophic and heterotrophic components of soil CO<sub>2</sub> flux, as well as respiration from woody biomass and foliage are shown in Table 1. Soil respiration represented the largest component of ecosystem respiration at  $810 \pm 48 \text{ g Cm}^{-2} \text{ yr}^{-1}$ . Estimates of soil respiration from manual chambers and autochambers were within 5% of one another and annual estimates were relatively insensitive to the type of model used to scale instantaneous measurements to annual fluxes (data not shown). Modelled winter fluxes from manual and autochambers were similar to estimates over the same time period using a soda lime technique (data not shown). Annual soil respiration estimates are also within the range estimated at similar stands elsewhere within the Bartlett Experimental Forest ( $790\text{--}864 \text{ g Cm}^{-2}\text{yr}^{-1}$ ; Bae et al., 2015).

The heterotrophic portion of soil respiration (using the partitioning approach described above) was estimated at  $434 \pm 101 \text{ g Cm}^{-2}\text{yr}^{-1}$ , and was the largest heterotrophic component of ecosystem respiration. In comparison, independent estimates of RSH from summing inputs of detritus were  $388 \text{ g Cm}^{-2}\text{yr}^{-1}$ . This value is within the uncertainty but lower than our estimates of RSH using the partitioning approach. In the ecosystem is roughly in steady state with regards to soil inputs and outputs, then estimates of RSH made by summing detrital inputs are likely underestimates because they exclude inputs from incorporation of CWD and root exudates. Heterotrophic respiration from aboveground dead woody biomass was estimated at  $61 \pm 12 \text{ g Cm}^{-2}\text{yr}^{-1}$ .

The autotrophic portion of soil respiration was the largest component of autotrophic ecosystem respiration (55%) at  $376 \pm 101 \text{ g Cm}^{-2}\text{yr}^{-1}$ . Autotrophic respiration from foliage and live woody material together make up 45% of total autotrophic respiration, estimated at  $149 \pm 20$  and  $153 \pm 114 \text{ g Cm}^{-2}\text{yr}^{-1}$ , respectively.

Measurements of the components of ecosystem respiration include soil respiration as well as aboveground foliar and woody respiration. We had measurements for total soil respiration and foliar respiration but lacked direct measurements of respiration from aboveground woody material. To assess the consistency of our estimates of aboveground woody respiration with estimates of other measured carbon fluxes in this system, we compared mean daily estimates of  $\text{Re}_{\text{EC}}$  to soil respiration ( $R_s$ ), to estimate respiration from aboveground components  $R_{\text{abv}}$ . The difference between mean annual  $\text{Re}_{\text{EC}}$  and  $R_s$  was  $343 \text{ g Cm}^{-2}\text{yr}^{-1}$ , or  $\sim 30\%$  of  $\text{Re}_{\text{EC}}$  (Fig. 3a). In comparison, the sum of our estimates of aboveground live foliar and woody autotrophic, as well as dead woody heterotrophic respiration from biometric estimates totaled  $363 \text{ g Cm}^{-2}\text{yr}^{-1}$ , roughly 31% of  $\text{Re}_{\text{EC}}$ .

### 3.2. Interannual variation and climate drivers

Considerable interannual variation in several meteorological and phenological variables occurred over the 13-year period (2004–2016) used to calculate mean C fluxes. For example, mean annual air temperature varied by nearly 2°C, mean spring (Julian days 76–135) and early summer (Julian days 136–215) air temperatures by more than 3°C, and mean winter air temperature by more than 6°C. Variables related to the start of the growing season also differed significantly over the 13-year period with variations in soil thaw day of more than a month, the onset of gross carbon uptake by more than 2 weeks, and the length of the vernal window by more than 5 weeks. In addition, growing season precipitation ranged from 279 to 680mm, while the number of growing season days with a mean volumetric water content (VWC) less than 17.5% ranged from 0 to 42 days per year.

Interannual variation in eddy covariance estimates of GPP,  $R_e$ , and NEP during this 13-year period varied by  $\pm 9\%$ ,  $\pm 12\%$ , and  $\pm 80\%$  around their means, respectively. We used stepwise multiple regression and model averaging to identify the phenological and meteorological parameters that were most strongly related to interannual variation in C fluxes (e.g. Hui et al., 2003). Using simple regression approaches, a majority of the interannual variation in  $GPP_{EC}$  were captured using a two-parameter model ( $r^2=0.83$   $p < 0.0001$ ) that included growing season soil temperature (negative correlation) and total incoming PAR during the growing season (positive correlation) - the two parameters that were used to parameterize the gap filling models employed for  $R_{eEC}$  and  $GPP_{EC}$ , respectively. Similarly, interannual variation in  $R_{eEC}$  was most strongly related to fluctuations in mean annual soil temperature (positive correlation).

Because of the predominance of gap-filled estimates in computing annual sums, we took a second approach to assess potential controls on interannual C flux variability using only high quality, half-hourly NEE data to parameterize a simple Michaelis-Menten light-response model. Interannual variation in modeled parameter estimates of canopy level maximum gross carbon uptake ( $A_{max}$ ) and dark respiration ( $R_d$ ) were regressed against meteorological and phenological variables.

The strongest correlation with growing season (June–August)  $A_{max}$ , was the length of the vernal window, defined here as the number of days between soil thaw and the start of the C uptake period ( $r^2=0.74$ ,  $p < 0.00031$ ; Fig. 4b). Taken separately, soil thaw day was also significantly, positively correlated with  $A_{max}$  ( $r^2=0.44$ ,  $p=0.019$ ; Fig. 4a), while the start of C uptake was not ( $p=0.12$ ). A longer vernal window (and an earlier soil thaw day) was correlated with a lower canopy  $A_{max}$ . Adding additional parameters did not result in an improved model and we did not detect a correlation between  $A_{max}$  and previous year net or gross C uptake at annual or seasonal time scales. Interannual variation in estimates of canopy-level dark respiration from the light-response model was positively correlated to  $A_{max}$  ( $r^2=0.69$ ,



$p=0.0009$ ), and, showed a similar negative correlation with the length of the vernal window ( $r^2=0.47$   $p=0.0014$ ).

Annual wood growth (Fig. 5a) was compared to both current-year and previous year meteorological and phenological variables as well as  $GPP_{EC}$  and  $NEP_{EC}$ , across a range of time periods (seasons). No significant relationship was detected between annual wood production and variations in gross or net carbon uptake from any time period (current-year or lagged). Instead wood growth was best predicted with a two parameter model that included early summer air temperature and the number of growing season days with soil volumetric water content less than 17.5% ( $r^2=0.75$ ,  $p < 0.002$ ,  $RMSE=16.9$   $g\ Cm^{-2}yr^{-1}$ ; Fig. 5b), with higher wood growth rates occurring in warmer and wetter years.

## 4. Discussion

### 4.1. Comparison of top-down and bottom-up approaches and uncertainty using mean C fluxes

Any technique for quantifying ecosystem-scale carbon dynamics has both strengths and limitations. Comparing top-down eddy covariance estimates of C exchange and bottom-up biometric estimates of C fluxes can serve as a valuable cross-validation tool, and can improve estimates of both an ecosystem's carbon balance as well as its components. At BEF, differences in 13year mean (2004–2016) estimates of NEP, GPP, and  $R_e$  between eddy covariance and biometric approaches were all within 10% of one another, indicating surprising consistency between methods despite large differences in their underlying sources of error. Consistency between eddy covariance and biometric approaches is often seen when comparing multiyear mean estimates. For example, at a secondary successional mixed northern hardwood forest in Michigan, the difference between NEP from eddy covariance and biometric approaches varied by up to 148% for individual years, but converged to within 1% of one another using 5year mean estimates (Gough et al., 2008).

The agreement in eddy covariance and biometric C flux estimates at BEF provided confidence in estimates of difficult-to-measure C fluxes, and highlighted the advantage of complementary methodological approaches. For example, the flux tower at BEF is situated within a valley at 250m above sea level, and on all sides the surrounding land rises to >750m above sea level within 3km of the flux tower (Fig. 1). This topographic relief increases the potential for advective transport of  $CO_2$ , which could lead to underestimates of C exchange measured at the top of the eddy covariance flux tower. Advective losses are a well-known challenge when using the eddy covariance technique and have been dealt with in several ways; the most common being the application of a  $u_{star}$  (friction velocity) threshold filter to exclude data when atmospheric turbulence is not developed enough to minimize horizontal advective transport (Aubinet, 2008; Aubinet et al., 2012). Following the  $u_{star}$  filter threshold selection approach of Barretal.

(2013), the high ustar threshold determined at BEF ( $0.5\text{ms}^{-1}$ ), in addition to other data gaps resulted in exclusion of >90% of available nighttime data (Fig. 2). Despite this tradeoff in data quantity, using only high quality, ustar filtered data, resulted in good agreement with biometric approaches.

The use of biometric data to estimate NEP, GPP, and  $R_e$  requires estimates of C flux to several ecosystem pools that are extremely difficult to measure. At BEF aboveground fluxes of net primary production are relatively well-constrained, while belowground C fluxes to fine roots and especially mycorrhizal fungi have higher uncertainty. However, not including estimates of these difficult-to-measure fluxes resulted in an inconsistency between biometric and eddy covariance estimates of gross and net C fluxes. In lieu of making individual estimates of fine root and mycorrhizal production, a mass balance approach to estimate total belowground carbon allocation (TBCA) described in (Davidson et al., 2002), can be used, although it does not distinguish between fine root and mycorrhizal fungi production. This approach assumes that soil carbon stocks are at or near steady state and requires only estimates of soil respiration and aboveground fine litterfall. At BEF, TBCA was estimated at  $656 \pm 54 \text{ g Cm}^{-2} \text{ yr}^{-1}$ , similar to estimates of the sum of coarse and fine root production, mycorrhizal production, and soil autotrophic respiration,  $644 \text{ g Cm}^{-2} \text{ yr}^{-1}$ .

Estimates of aboveground foliar and woody respiration are also difficult to constrain given their biological control and temporal heterogeneity. The difference between estimates of ecosystem respiration and soil respiration is a mass balance approach that can estimate respiration of aboveground ecosystem components (Giasson et al., 2013). At BEF, this approach yielded similar results ( $343 \text{ g Cm}^{-2} \text{ yr}^{-1}$ ) to our initial estimates of aboveground respiration ( $363 \pm 117 \text{ g Cm}^{-2} \text{ yr}^{-1}$ ). This mass balance approach also yields estimates at a fine temporal resolution and may capture important phenological events (Davidson et al., 2006). At BEF estimates of  $R_{abv}$  using this mass balance approach highlight the phenological influence on aboveground respiration, with  $R_{abv}$  contributing a relatively large proportion of  $R_e$  during spring leaf out (and the onset of wood growth) and during autumn leaf senescence (Fig. 3b).

The consistency of our initial C flux estimates with mass balance approaches that used soil respiration, aboveground litterfall, and  $R_{eEC}$  to calculate TBCA and  $R_{abv}$ , demonstrate the benefit of including these as routine data streams at eddy covariance network sites. Including soil respiration and litterfall measurements at flux sites provides valuable information on both above and belowground ecosystem C fluxes allowing for not only cross validation of ecosystem C fluxes but the ability to more rigorously test ecosystem models (McFarlane et al., 2014; Phillips et al., 2017).

## 4.2. Interannual variation

### 4.2.1. GPP, $R_e$ , $A_{max}$

Interannual variations in GPP, Re, NEP, and parameters describing light response functions are determined by both direct and indirect drivers, and have the potential to provide insight into how ecosystems might respond under future climate. A complication in understanding the drivers of interannual C variation from eddy covariance is the abundance of gap-filled data. At BEF, on average, 90–95% of nighttime and nearly 50% of daytime fluxes during the growing season were gap-filled. It is thus not surprising that interannual variation in gap-filled  $GPP_{EC}$  and  $Re_{EC}$  were strongly related to temperature and incoming PAR, the two variables used to parameterize the gap-filling models.

Although short term (hours to days) changes in temperature and PAR are frequently correlated to short term variations in C fluxes (and hence why they are used in gap-filling models), they may not be directly related to interannual variation in C fluxes. Several studies have shown the importance of variation in the biotic response to abiotic drivers, especially for regulating interannual carbon flux variation (Richardson et al., 2007). Data from BEF support a similar conclusion. For example, using only high-quality, raw (not gap-filled) data, the strong relationship between growing season canopy  $A_{max}$  (and  $R_d$ ) and the length of the vernal window suggests that indirect mechanisms (biotic responses) are important in regulating canopy C exchange.

Mechanisms through which the length of the vernal window can influence canopy photosynthesis are not well understood. In the northeastern US, a longer vernal window has been correlated to winters with a reduced snowpack (Contosta et al., 2016). Other studies have repeatedly linked reduced snowpack to an increase in soil freeze-thaw events and increases in the loss of nutrients through both dissolved and gaseous pathways (Matzner and Borken, 2008; Song et al., 2017). For example, at the Hubbard Brook Experimental Forest (40km west of BEF), both experimental (Campbell et al., 2014; Fitzhugh et al., 2001) and observational studies across a climate gradient (Durán et al., 2016) have shown increased losses of nitrogen and decreased N availability following winters with reduced snowpack. Whether decreases in soil nutrient availability prior to leaf out results in decreased foliar biomass, lower canopy nitrogen content, or reduced photosynthetic capacity is still unknown. However, leaf area index (LAI) is often limited by soil nutrients and water (Cowling and Field, 2003), and numerous studies have shown significant increases in foliar biomass and LAI following fertilization, e.g. Gower et al. (1992).

In addition to reductions in nutrient availability, earlier snowmelt has been shown to intensify forest hydrological cycles and increase springtime runoff (Creed et al., 2015). Late growing season water stress related to earlier snowmelt has also been suggested as the driver of decreases in peak growing season productivity in boreal forests (Buermann et al., 2013) and temperate forests of the western US (Hu et al., 2010). At BEF the length of the vernal window is negatively correlated to soil moisture during the month

prior to leaf out ( $r^2=0.40$ ,  $p=0.027$ ) but not to soil moisture during the late growing season ( $r^2=0.17$ ,  $p=0.16$ ). Although mechanisms relating growing season Amax to the length of the vernal window are not fully known, data from BEF suggest that winter and spring conditions can exert a strong influence over ecosystem C dynamics during the growing season.

A few studies in temperate forests have found lagged effects on C fluxes (e.g. Howland Experimental Forest, Maine; (Richardson et al., 2013)). At BEF we did not detect a correlation between prior year meteorological conditions or C uptake, with current year C fluxes. In other work at BEF, Carbone et al., (2013) found that in stem wood of *Acer rubrum* trees, the nonstructural carbohydrate pool included both fast (younger) and slow (older) cycling subpools that could support growth and respiration of woody tissues. The lack of a correlation we see between wood growth and prior year climate and C fluxes may in part be the result of the growth habit of foliage of tree species at BEF. At BEF foliage and new shoots of the majority of the dominant species within the flux tower footprint have an indeterminate growth habit, meaning that during and after spring leaf expansion from the winter bud, the shoot apex remains active and continues to initiate additional leaves and shoot internodes if conditions are favorable. Of the dominant species only American beech and sugar maple tend to have determinate type foliar and shoot growth, where the number of leaf buds (number of leaves) is determined at the end of the preceding growing season. Many ecosystem models allocate C to foliar growth based more on a determinant type growth.

#### 4.2.2. Wood growth

Despite the importance of wood growth for a variety of ecosystem services, we still do not fully understand the mechanisms controlling variability in wood growth and how they may respond under future climate scenarios. Evidence from broad-scale analyses suggest a tradeoff between C allocation to wood versus fine roots, reflecting a tradeoff between acquiring growth limiting nutrients and/or water and competition for space in the sunlit canopy (Dybzinski et al., 2011; Litton et al., 2007). Whether this tradeoff at ecosystem scales occurs interannually within an ecosystem is unknown.

Alternatively, wood growth is often viewed as “source” (C supply) versus “sink” (C demand) limited (Körner, 2015). At broad spatial scales wood growth generally correlates to GPP (Litton et al., 2007). This is why wood growth in many terrestrial ecosystem models is primarily source-driven, where wood production is linked to the amount of gross photosynthesis. However, recent work has downplayed the importance of C source in controlling wood growth and has emphasized the importance of climatically sink-driven metabolic and phenological processes (Delpierre et al., 2016, 2015; Guillemot et al., 2015; Körner, 2003). These studies indicate an earlier onset of xylogenesis, faster rates of cell division, and faster rates of cell division under warmer, wetter conditions.

Our inability to detect a correlation between wood growth and either GPP or NEP at BEF suggests that interannual variations in wood growth are likely not directly “source driven.” Instead, wood growth is more strongly related to early growing season air temperature and growing season soil water stress. At BEF, wood growth was higher during years with warmer air temperatures during the early growing season and in years with ample growing season soil moisture, consistent with metabolic/phenologically “sink” driven mechanisms. Further, at BEF Carbone et al. (2013) showed the importance of stored C to the growth and metabolism of woody biomass, indicating that C allocated towards wood growth relies on both recent photosynthate as well as internal reserve C pools derived from both older and recent photosynthates. At broad-scales allocation to wood growth is likely controlled by C source (GPP) as well as tradeoffs involved in acquiring growth limiting nutrients, while metabolically driven mechanisms may be important in regulating interannual variability within a site.

## 5. Conclusion

Long-term dataset using multiple approaches to estimate ecosystem carbon fluxes can provide cross validation of difficult-to-measure fluxes as well as potential insight into mechanisms that may be regulating C fluxes. At BEF, top-down and bottom-up approaches to estimate gross and net C exchange agreed well at a multiyear scale and provided more confidence in several difficult-to-measure C fluxes such as aboveground components of ecosystem respiration and belowground allocation to mycorrhizal fungi. The results from BEF also suggest several potential relationships that may be important to understanding forest ecosystem C fluxes under future climate. These include potential indirect effects of winter and spring climate (vernal window) on growing season photosynthesis, as well as direct metabolic (sink-driven) mechanisms driven by growing season climate. Such mechanisms warrant future study to assess their importance and to allow for their potential inclusion in models aimed at predicting ecosystem C dynamics under future conditions.

## Acknowledgements

Research at the Bartlett Experimental Forest is supported by the USDA Forest Service’s Northern Research Station. We acknowledge funding support from the following grants: National Science Foundation awards #DEB-1114804, #1638688, and # 1114804; Northeastern States Research Cooperative #12DG11242307065; Hubbard Brook Long Term Ecological Research program, NSF1114804; NH EPSCoR Program NSF Research Infrastructure Improvement Award# EPS 1101245; NASA Carbon Cycle Science Awards #NNX08AG14G and #NNX14AJ18G; NASA Terrestrial Ecology Award #NNX11AB88G. TFK was supported by the Director, Office of Science, Office of Biological and Environmental Research of the US Department of Energy under Contract DE-AC02-05CH11231 as part of the RGCM BGC-Climate Feedbacks SFA. We also acknowledge the staff at Bartlett

Experimental Forest, in particular Chris Costello, as well as the invaluable assistance of numerous students over the last 13 years.

## References

Aubinet, M., 2008. Eddy covariance Co<sub>2</sub> flux measurements in nocturnal conditions: an analysis of the problem. *Ecol. Appl.* 18, 1368–1378. <http://dx.doi.org/10.1890/061336.1>.

Aubinet, M., Feigenwinter, C., Heinesch, B., Laffineur, Q., Papale, D., Reichstein, M., Rinne, J., Gorsel, E.V., 2012. Nighttime flux correction. In: Aubinet, M., Vesala, T., Papale, D. (Eds.), *Eddy Covariance*, Springer Atmospheric Sciences. Springer, Netherlands, pp. 133–157. [http://dx.doi.org/10.1007/978-94-007-2351-1\\_5](http://dx.doi.org/10.1007/978-94-007-2351-1_5).

Bae, K., Fahey, T.J., Yanai, R.D., Fisk, M., 2015. Soil nitrogen availability affects belowground carbon allocation and soil respiration in Northern Hardwood Forests of New Hampshire. *Ecosystems* 1–13. <http://dx.doi.org/10.1007/s10021-015-9892-7>.

Barr, A.G., Black, T.A., Hogg, E.H., Kljun, N., Morgenstern, K., Nesic, Z., 2004. Interannual variability in the leaf area index of a boreal aspen-hazelnut forest in relation to net ecosystem production. *Agric. For. Meteorol.* 126, 237–255. <http://dx.doi.org/10.1016/j.agrformet.2004.06.011>.

Barr, A.G., Richardson, A.D., Hollinger, D.Y., Papale, D., Arain, M.A., Black, T.A., Bohrer, G., Dragoni, D., Fischer, M.L., Gu, L., Law, B.E., Margolis, H.A., McCaughey, J.H., Munger, J.W., Oechel, W., Schaeffer, K., 2013. Use of change-point detection for friction-velocity threshold evaluation in eddy-covariance studies. *Agric. For. Meteorol.* 171–172, 31–45. <http://dx.doi.org/10.1016/j.agrformet.2012.11.023>.

Bernier, P., Hanson, P.J., Curtis, P.S., 2008. Measuring litterfall and branchfall. In: Hoover, C.M. (Ed.), *Field Measurements for Forest Carbon Monitoring*. Springer, Netherlands, pp. 91–101. [http://dx.doi.org/10.1007/978-1-4020-8506-2\\_7](http://dx.doi.org/10.1007/978-1-4020-8506-2_7).

Bond-Lamberty, B., Thomson, A., 2014. A Global Database of Soil Respiration Data, Version 3.0. Oak Ridge Natl. Lab. Distrib. Act. Arch. Cent., Oak Ridge Tenn. USA Data Set Available - Line [Http://daacornl.gov](http://daacornl.gov) [Http://dx.doi.org/10.3334/ORNLDAAC1235](http://dx.doi.org/10.3334/ORNLDAAC1235).

Bond-Lamberty, B., Wang, C., Gower, S.T., 2004. A global relationship between the heterotrophic and autotrophic components of soil respiration? *Glob. Change Biol.* 10, 1756–1766. <http://dx.doi.org/10.1111/j.1365-2486.2004.00816.x>.

Buermann, W., Bikash, P.R., Jung, M., Burn, D.H., Reichstein, M., 2013. Earlier springs decrease peak summer productivity in North American boreal forests. *Environ. Res. Lett.* 8, 024027. <http://dx.doi.org/10.1088/1748-9326/8/2/024027>.

- Campbell, J.L., Soggiu, A.M., Templer, P.H., 2014. Increased nitrogen leaching following soil freezing is due to decreased root uptake in a northern hardwood forest. *Glob. Change Biol.* 20, 2663–2673. <http://dx.doi.org/10.1111/gcb.12532>.
- Carbone, M.S., Czimczik, C.I., Keenan, T.F., Murakami, P.F., Pederson, N., Schaberg, P.G., Xu, X., Richardson, A.D., 2013. Age, allocation and availability of nonstructural carbon in mature red maple trees. *New Phytol.* 200, 1145–1155. <http://dx.doi.org/10.1111/nph.12448>.
- Caspersen, J.P., Pacala, S.W., Jenkins, J.C., Hurtt, G.C., Moorcroft, P.R., Birdsey, R.A., 2000. Contributions of land-use history to carbon accumulation in U.S. For. Sci. 290, 1148–1151. <http://dx.doi.org/10.1126/science.290.5494.1148>.
- Chapin III, F.S., Woodwell, G.M., Randerson, J.T., Rastetter, E.B., Lovett, G.M., Baldocchi, D.D., Clark, D.A., Harmon, M.E., Schimel, D.S., Valentini, R., Wirth, C., Aber, J.D., Cole, J.J., Goulden, M.L., Harden, J.W., Heimann, M., Howarth, R.W., Matson, P.A., McGuire, A.D., Melillo, J.M., Mooney, H.A., Neff, J.C., Houghton, R.A., Pace, M.L., Ryan, M.G., Running, S.W., Sala, O.E., Schlesinger, W.H., Schulze, E.-D., 2006. Reconciling carbon-cycle concepts, terminology, and methods. *Ecosystems* 9, 1041–1050. <http://dx.doi.org/10.1007/s10021-005-0105-7>.
- Chojnacky, D.C., Heath, L.S., Jenkins, J.C., 2014. Updated generalized biomass equations for North American tree species. *Forestry* 87, 129–151. <http://dx.doi.org/10.1093/forestry/cpt053>.
- Chojnacky, D.C., Milton, M., 2008. Measuring carbon in shrubs. In: Hoover, C.M. (Ed.), *Field Measurements for Forest Carbon Monitoring*. Springer, Netherlands, pp. 45–72. [http://dx.doi.org/10.1007/978-1-4020-8506-2\\_5](http://dx.doi.org/10.1007/978-1-4020-8506-2_5).
- Clark, D.A., Brown, S., Kicklighter, D.W., Chambers, J.Q., Thomlinson, J.R., Ni, J., 2001. Measuring net primary production in forests: concepts and field methods. *Ecol. Appl.* 11, 356–370. [http://dx.doi.org/10.1890/1051-0761\(2001\)011\[0356:MNPPIF\]2.0.CO;2](http://dx.doi.org/10.1890/1051-0761(2001)011[0356:MNPPIF]2.0.CO;2).
- Contosta, A.R., Adolph, A., Burchsted, D., Burakowski, E., Green, M., Guerra, D., Albert, M., Dibb, J., Martin, M., McDowell, W.H., Routhier, M., Wake, C., Whitaker, R., Wollheim, W., 2016. A longer vernal window: the role of winter coldness and snowpack in driving spring transitions and lags. *Glob. Change Biol.* <http://dx.doi.org/10.1111/gcb.13517>. n/a-n/a.
- Cowling, S.A., Field, C.B., 2003. Environmental control of leaf area production: implications for vegetation and land-surface modeling. *Glob. Biogeochem. Cycles* 17, 1007. <http://dx.doi.org/10.1029/2002GB001915>.
- Creed, I.F., Hwang, T., Lutz, B., Way, D., 2015. Climate warming causes intensification of the hydrological cycle, resulting in changes to the vernal and autumnal windows in a northern temperate forest. *Hydrol. Process.* 29, 3519–3534. <http://dx.doi.org/10.1002/hyp.10450>.

Curtis, P.S., 2008. Estimating aboveground carbon in live and standing dead trees. In: Hoover, C.M. (Ed.), *Field Measurements for Forest Carbon Monitoring*. Springer, Netherlands, pp. 39–44. [http://dx.doi.org/10.1007/978-1-4020-8506-2\\_4](http://dx.doi.org/10.1007/978-1-4020-8506-2_4).

Davidson, E.A., Richardson, A.D., Savage, K.E., Hollinger, D.Y., 2006. A distinct seasonal pattern of the ratio of soil respiration to total ecosystem respiration in a sprucedominated forest. *Glob. Change Biol.* 12, 230–239. <http://dx.doi.org/10.1111/j.1365-2486.2005.01062.x>.

Davidson, E.A., Savage, K., Bolstad, P., Clark, D.A., Curtis, P.S., Ellsworth, D.S., Hanson, P.J., Law, B.E., Luo, Y., Pregitzer, K.S., Randolph, J.C., Zak, D., 2002. Belowground carbon allocation in forests estimated from litterfall and IRGA-based soil respiration measurements. *Agric. For. Meteorol. FLUXNET 2000 Synth.* 113, 39–51. [http://dx.doi.org/10.1016/S0168-1923\(02\)00101-6](http://dx.doi.org/10.1016/S0168-1923(02)00101-6).

Delpierre, N., Berveiller, D., Granda, E., Dufrêne, E., 2016. Wood phenology, not carbon input, controls the interannual variability of wood growth in a temperate oak forest. *New Phytol.* 210, 459–470. <http://dx.doi.org/10.1111/nph.13771>.

Delpierre, N., Vitasse, Y., Chuine, I., Guillemot, J., Bazot, S., Rutishauser, T., Rathgeber, C.B.K., 2015. Temperate and boreal forest tree phenology: from organ-scale processes to terrestrial ecosystem models. *Ann. For. Sci.* 73, 5–25. <http://dx.doi.org/10.1007/s13595-015-0477-6>.

Domke, G.M., Woodall, C.W., Smith, J.E., 2011. Accounting for density reduction and structural loss in standing dead trees: implications for forest biomass and carbon stock estimates in the United States. *Carbon Balance Manag.* 6, 14. <http://dx.doi.org/10.1186/1750-0680-6-14>.

Durán, J., Morse, J.L., Groffman, P.M., Campbell, J.L., Christenson, L.M., Driscoll, C.T., Fahey, T.J., Fisk, M.C., Likens, G.E., Melillo, J.M., Mitchell, M.J., Templer, P.H., Vadeboncoeur, M.A., 2016. Climate change decreases nitrogen pools and mineralization rates in northern hardwood forests. *Ecosphere* 7 <http://dx.doi.org/10.1002/ecs2.1251>. n/a-n/a.

Dybzinski, R., Farrior, C., Wolf, A., Reich, P.B., Pacala, S.W., 2011. Evolutionarily stable strategy carbon allocation to foliage, wood, and fine roots in trees competing for light and nitrogen: an analytically tractable, individual-based model and quantitative comparisons to data. *Am. Nat.* 177, 153–166. <http://dx.doi.org/10.1086/657992>.

Fitzhugh, R.D., Driscoll, C.T., Groffman, P.M., Tierney, G.L., Fahey, T.J., Hardy, J.P., 2001. Effects of soil freezing disturbance on soil solution nitrogen, phosphorus, and carbon chemistry in a northern hardwood ecosystem. *Biogeochemistry* 56, 215–238. <http://dx.doi.org/10.1023/A:1013076609950>.

Foster, D.R., Aber, J., 2004. *Forests in Time. Ecosystem Structure and Function as a Consequence of 1000 Years of Change.* Synthesis volume of



the Harvard Forest LTER Program. Yale University Press, New Haven, Connecticut, USA.

Giasson, M.-A., Ellison, A.M., Bowden, R.D., Crill, P.M., Davidson, E.A., Drake, J.E., Frey, S.D., Hadley, J.L., Lavine, M., Melillo, J.M., Munger, J.W., Nadelhoffer, K.J., Nicoll, L., Ollinger, S.V., Savage, K.E., Steudler, P.A., Tang, J., Varner, R.K., Wofsy, S.C., Foster, D.R., Finzi, A.C., 2013. Soil respiration in a northeastern US temperate forest: a 22-year synthesis. *Ecosphere* 4, 1–28. <http://dx.doi.org/10.1890/ES13.00183.1>.

Goodale, C.L., Apps, M.J., Birdsey, R.A., Field, C.B., Heath, L.S., Houghton, R.A., Jenkins, J.C., Kohlmaier, G.H., Kurz, W., Liu, S., Nabuurs, G.-J., Nilsson, S., Shvidenko, A.Z., 2002. Forest carbon sinks in the northern hemisphere. *Ecol. Appl.* 12, 891–899. [http://dx.doi.org/10.1890/1051-0761\(2002\)012\[0891:FCSITN\]2.0.CO;2](http://dx.doi.org/10.1890/1051-0761(2002)012[0891:FCSITN]2.0.CO;2).

Gough, C.M., Vogel, C.S., Schmid, H.P., Su, H.-B., Curtis, P.S., 2008. Multi-year convergence of biometric and meteorological estimates of forest carbon storage. *Chequamegon ecosystem-atmosphere study special issue: ecosystem-atmosphere carbon and water cycling in the temperate Northern Forests of the Great Lakes Region* Great Lakes Region Special issue. *Agric. For. Meteorol.* 148, 158–170. <http://dx.doi.org/10.1016/j.agrformet.2007.08.004>.

Gower, S.T., Vogt, K.A., Grier, C.C., 1992. Carbon dynamics of Rocky Mountain Douglas Fir: influence of Water and nutrient availability. *Ecol. Monogr.* 62, 43–65. <http://dx.doi.org/10.2307/2937170>.

Grogan, P., 1998. Co<sub>2</sub> flux measurement using soda lime: correction for water formed during co<sub>2</sub> adsorption. *Ecology* 79, 1467–1468. [http://dx.doi.org/10.1890/00129658\(1998\)079\[1467:CFMUSL\]2.0.CO;2](http://dx.doi.org/10.1890/00129658(1998)079[1467:CFMUSL]2.0.CO;2).

Guillemot, J., Martin-StPaul, N.K., Dufrêne, E., François, C., Soudani, K., Ourcival, J.M., Delpierre, N., 2015. The dynamic of the annual carbon allocation to wood in European tree species is consistent with a combined source–sink limitation of growth: implications for modelling. *Biogeosciences* 12, 2773–2790.

Harmon, M.E., Woodall, C.W., Fasth, B., Sexton, J., 2008. Woody Detritus Density and Density Reduction Factors for Tree Species in the United States: a Synthesis.

Harmon, M.E., Woodall, C.W., Fasth, B., Sexton, J., Yatkov, M., 2011. Differences between Standing and Downed Dead Tree Wood Density Reduction Factors: A Comparison Across Decay Classes and Tree Species.

Hobbie, E.A., Hobbie, J.E., 2008. Natural abundance of <sup>15</sup>N in nitrogen-limited forests and tundra can estimate nitrogen cycling through mycorrhizal fungi: a review. *Ecosystems* 11 (815). <http://dx.doi.org/10.1007/s10021-008-9159-7>.

Hollinger, D.Y., 2008. Defining a landscape-scale monitoring tier for the North American carbon program. In: Hoover, C.M. (Ed.), *Field Measurements for Forest Carbon Monitoring*. Springer, Netherlands, pp. 3–16.  
[http://dx.doi.org/10.1007/978-14020-8506-2\\_1](http://dx.doi.org/10.1007/978-14020-8506-2_1).

Hollinger, D.Y., Aber, J., Dail, B., Davidson, E.A., Goltz, S.M., Hughes, H., Leclerc, M.Y., Lee, J.T., Richardson, A.D., Rodrigues, C., Scott, N., Achuatavari, D., Walsh, J., 2004. Spatial and temporal variability in forest-atmosphere CO<sub>2</sub> exchange. *Glob. Change Biol.* 10, 1689–1706.  
<http://dx.doi.org/10.1111/j.1365-2486.2004.00847.x>.

Hu, J., Moore, D.J.P., Burns, S.P., Monson, R.K., 2010. Longer growing seasons lead to less carbon sequestration by a subalpine forest. *Glob. Change Biol.* 16, 771–783. <http://dx.doi.org/10.1111/j.1365-2486.2009.01967.x>.

Hui, D., Luo, Y., Katul, G., 2003. Partitioning inter annual variability in net ecosystem exchange between climatic variability and functional change. *Tree Physiol.* 23, 433–442.

Keith, H., Wong, S.C., 2006. Measurement of soil CO<sub>2</sub> efflux using soda lime absorption: both quantitative and reliable. *Soil Biol. Biochem.* 38, 1121–1131.  
<http://dx.doi.org/10.1016/j.soilbio.2005.09.012>.

Körner, C., 2015. Paradigm shift in plant growth control. *Curr. Opin. Plant Biol.* 25, 107–114. <http://dx.doi.org/10.1016/j.pbi.2015.05.003>.

Körner, C., 2003. Carbon limitation in trees. *J. Ecol.* 91, 4–17.  
<http://dx.doi.org/10.1046/j.1365-2745.2003.00742.x>.

Litton, C.M., Raich, J.W., Ryan, M.G., 2007. Carbon allocation in forest ecosystems. *Glob. Change Biol.* 13, 2089–2109.  
<http://dx.doi.org/10.1111/j.1365-2486.2007.01420.x>.

Luyssaert, S., Schulze, E.-D., Börner, A., Knohl, A., Hessenmöller, D., Law, B.E., Ciais, P., Grace, J., 2008. Old-growth forests as global carbon sinks. *Nature* 455, 213–215. <http://dx.doi.org/10.1038/nature07276>.

Matzner, E., Borren, W., 2008. Do freeze-thaw events enhance C and N losses from soils of different ecosystems? A review. *Eur. J. Soil Sci.* 59, 274–284. <http://dx.doi.org/10.1111/j.1365-2389.2007.00992.x>.

McFarlane, K., Finzi, A., Nave, L., Tang, J., 2014. Recommendations for Belowground Carbon Data and Measurements for the AmeriFlux Network [WWW Document]. ISCN Accessed 18 April 17.  
<http://iscn.fluxdata.org/community/publication/recommendations-for-belowground-carbon-data-and-measurements-for-theameriflux-network/>.

Novick, K., Brantley, S., Miniati, C.F., Walker, J., Vose, J.M., 2014. Inferring the contribution of advection to total ecosystem scalar fluxes over a tall forest in complex terrain. *Agric. For. Meteorol.* 185, 1–13.  
<http://dx.doi.org/10.1016/j.agrformet.2013.10.010>.

- Odum, E.P., 1969. The strategy of ecosystem development. *Science* 164, 262–270. [http:// dx.doi.org/10.1126/science.164.3877.262](http://dx.doi.org/10.1126/science.164.3877.262).
- Ollinger, S.V., Smith, M.L., Martin, M.E., Hallett, R.A., Goodale, C.L., Aber, J.D., 2002. Regional variation in foliar chemistry and N cycling among forests of diverse history and composition. *Ecology* 83, 339–355. <http://dx.doi.org/10.2307/2680018>.
- Quimette, A., Guo, D., Hobbie, E., Gu, J., 2013. Insights into root growth, function, and mycorrhizal abundance from chemical and isotopic data across rootorders. *Plant Soil* 367, 313–326. <http://dx.doi.org/10.1007/s11104-012-1464-4>.
- Park, B.B., Yanai, R.D., Vadeboncoeur, M.A., Hamburg, S.P., 2007. Estimating root biomass in rocky soils using pits, cores, and allometric equations. *Soil Sci. Soc. Am. J.* 71, 206–213. <http://dx.doi.org/10.2136/sssaj2005.0329>.
- Pesonen, A., Leino, O., Maltamo, M., Kangas, A., 2009. Comparison of field sampling methods for assessing coarse woody debris and use of airborne laser scanning as auxiliary information. *For. Ecol. Manag.* 257, 1532–1541. <http://dx.doi.org/10.1016/j.foreco.2009.01.009>.
- Phillips, C.L., Bond-Lamberty, B., Desai, A.R., Lavoie, M., Risk, D., Tang, J., Todd-Brown, K., Vargas, R., 2017. The value of soil respiration measurements for interpreting and modeling terrestrial carbon cycling. *Plant Soil* 413, 1–25. <http://dx.doi.org/10.1007/s11104-016-3084-x>.
- Phillips, S.C., Varner, R.K., Frohling, S., Munger, J.W., Bubier, J.L., Wofsy, S.C., Crill, P.M., 2010. Interannual, seasonal, and diel variation in soil respiration relative to ecosystem respiration at a wetland to upland slope at Harvard Forest. *J. Geophys. Res. Biogeosci.* 115, G02019. <http://dx.doi.org/10.1029/2008JG000858>.
- Post, W.M., Kwon, K.C., 2000. Soil carbon sequestration and land-use change: processes and potential. *Glob. Change Biol.* 6, 317–327. <http://dx.doi.org/10.1046/j.13652486.2000.00308.x>.
- Potter, D., Obbard, M., Howe, E., 2015. Ontario Wildlife Food Survey, 2014. Ont. Minist. Nat. Resour. For. Sci. Res. Branch Peterb. Ont. Sci. Res. Tech. Rep. TR-01.
- Raich, J.W., Nadelhoffer, K.J., 1989. Belowground carbon allocation in forest ecosystems: global trends. *Ecology* 70, 1346–1354. <http://dx.doi.org/10.2307/1938194>.
- Richardson, A.D., Braswell, B.H., Hollinger, D.Y., Burman, P., Davidson, E.A., Evans, R.S., Flanagan, L.B., Munger, J.W., Savage, K., Urbanski, S.P., Wofsy, S.C., 2006. Comparing simple respiration models for eddy flux and dynamic chamber data. *Agric. For. Meteorol.* 141, 219–234. <http://dx.doi.org/10.1016/j.agrformet.2006.10.010>.

- Richardson, A.D., Carbone, M.S., Keenan, T.F., Czimczik, C.I., Hollinger, D.Y., Murakami, P., Schaberg, P.G., Xu, X., 2013. Seasonal dynamics and age of stemwood nonstructural carbohydrates in temperate forest trees. *New Phytol.* 197, 850–861. <http://dx.doi.org/10.1111/nph.12042>.
- Richardson, A.D., Hollinger, D.Y., 2007. A method to estimate the additional uncertainty in gap-filled NEE resulting from long gaps in the CO<sub>2</sub> flux record. *Agric. For. Meteorol.* 147, 199–208. <http://dx.doi.org/10.1016/j.agrformet.2007.06.004>.
- Richardson, A.D., Hollinger, D.Y., Aber, J.D., Ollinger, S.V., Braswell, B.H., 2007. Environmental variation is directly responsible for short- but not long-term variation in forest-atmosphere carbon exchange. *Glob. Change Biol.* 13, 788–803. <http://dx.doi.org/10.1111/j.1365-2486.2007.01330.x>.
- Russell, M.B., Woodall, C.W., Fraver, S., D'Amato, A.W., Domke, G.M., Skog, K.E., 2014. Residence times and decay rates of downed woody debris biomass/carbon in Eastern US Forests. *Ecosystems* 17, 765–777. <http://dx.doi.org/10.1007/s10021-0149757-5>.
- Smith, M.-L., Hollinger, D.Y., Ollinger, S., 2008. Estimation of Forest canopy nitrogen concentration. In: Hoover, C.M. (Ed.), *Field Measurements for Forest Carbon Monitoring*. Springer, Netherlands, pp. 197–203. [http://dx.doi.org/10.1007/978-14020-8506-2\\_15](http://dx.doi.org/10.1007/978-14020-8506-2_15).
- Song, Y., Zou, Y., Wang, G., Yu, X., 2017. Altered soil carbon and nitrogen cycles due to the freeze-thaw effect: a meta-analysis. *Soil Biol. Biochem.* 109, 35–49. <http://dx.doi.org/10.1016/j.soilbio.2017.01.020>.
- Thomas, S.C., Martin, A.R., 2012. Carbon content of tree tissues: a synthesis. *Forests* 3, 332–352. <http://dx.doi.org/10.3390/f3020332>.
- Tjoelker, M.G., Oleksyn, J., Reich, P.B., 2001. Modelling respiration of vegetation: evidence for a general temperature-dependent Q<sub>10</sub>. *Glob. Change Biol.* 7, 223–230. <http://dx.doi.org/10.1046/j.1365-2486.2001.00397.x>.
- Vadeboncoeur, M.A., Hamburg, S.P., Blum, J.D., Pennino, M.J., Yanai, R.D., Johnson, C.E., 2012. The quantitative soil pit method for measuring belowground carbon and nitrogen stocks. *Soil Sci. Soc. Am. J.* 76, 2241–2255. <http://dx.doi.org/10.2136/sssaj2012.0111>.
- Vadeboncoeur, M.A., Hamburg, S.P., Yanai, R.D., Blum, J.D., 2014. Rates of sustainable forest harvest depend on rotation length and weathering of soil minerals. *For. Ecol. Manag.* 194–205. <http://dx.doi.org/10.1016/j.foreco.2014.01.012>.
- Valentine, H.T., Gove, J.H., Ducey, M.J., Gregoire, T.G., Williams, M.S., 2008. Estimating the carbon in coarse woody debris with perpendicular distance sampling. In: Hoover, C.M. (Ed.), *Field Measurements for Forest Carbon*

Monitoring. Springer, Netherlands, pp. 73–87. [http://dx.doi.org/10.1007/978-1-4020-8506-2\\_6](http://dx.doi.org/10.1007/978-1-4020-8506-2_6).

van Gorsel, E., Delpierre, N., Leuning, R., Black, A., Munger, J.W., Wofsy, S., Aubinet, M., Feigenwinter, C., Beringer, J., Bonal, D., Chen, B., Chen, J., Clement, R., Davis, K.J., Desai, A.R., Dragoni, D., Etzold, S., Grünwald, T., Gu, L., Heinesch, B., Hutya, L.R., Jans, W.W.P., Kutsch, W., Law, B.E., Leclerc, M.Y., Mammarella, I., Montagnani, L., Noormets, A., Rebmann, C., Wharton, S., 2009. Estimating nocturnal ecosystem respiration from the vertical turbulent flux and change in storage of CO<sub>2</sub>. Special section on Water and carbon dynamics in selected ecosystems in China. *Agric. For. Meteorol.* 149, 1919–1930. <http://dx.doi.org/10.1016/j.agrformet.2009.06.020>.

Vickers, D., Irvine, J., Martin, J.G., Law, B.E., 2012. Nocturnal subcanopy flow regimes and missing carbon dioxide. *Agric. For. Meteorol.* 152, 101–108. <http://dx.doi.org/10.1016/j.agrformet.2011.09.004>.

Whittaker, R.H., Bormann, F.H., Likens, G.E., Siccama, T.G., 1974. The Hubbard Brook Ecosystem Study: forest biomass and production. *Ecol. Monogr.* 44, 233–254. <http://dx.doi.org/10.2307/1942313>.

Yanai, R.D., Battles, J.J., Richardson, A.D., Blodgett, C.A., Wood, D.M., Rastetter, E.B., 2010. Estimating uncertainty in ecosystem budget calculations. *Ecosystems* 13, 239–248. <http://dx.doi.org/10.1007/s10021-010-9315-8>.

Yanai, R.D., Vadeboncoeur, M.A., Hamburg, S.P., Arthur, M.A., Fuss, C.B., Groffman, P.M., Siccama, T.G., Driscoll, C.T., 2013. From missing source to missing sink: longterm changes in the nitrogen budget of a Northern Hardwood Forest. *Environ. Sci. Technol.* 47, 11440–11448. <http://dx.doi.org/10.1021/es4025723>.

Young, H.E., Ribe, J.H., Wainwright, K., 1980. Weight Tables for Tree and Shrub Species in Maine. Maine Life Sciences and Agriculture Experiment Station Miscellaneous Report USA.

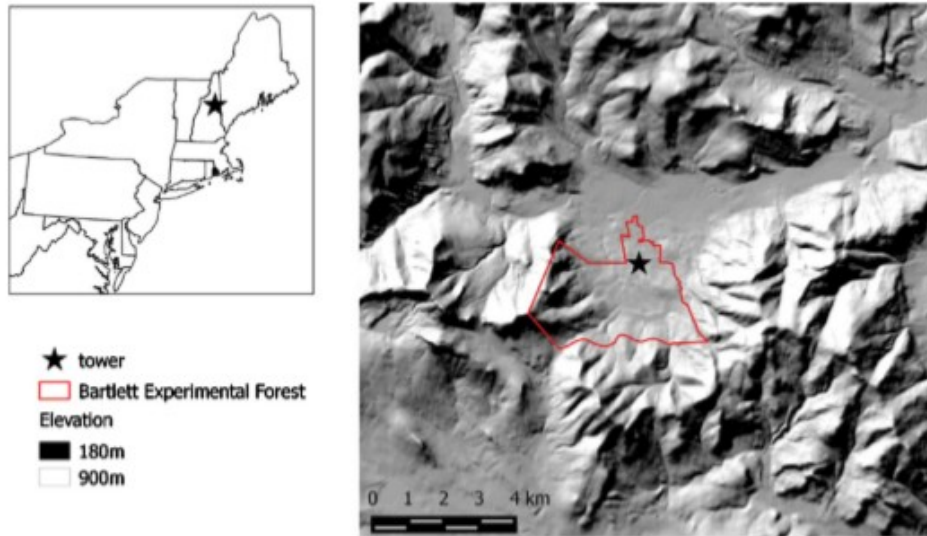
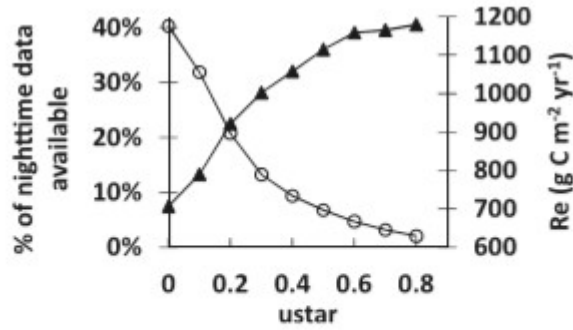


Fig. 1. A) Location of Bartlett Experimental Forest (BEF); B) Representation of topography surrounding BEF.

**Table 1**  
Mean carbon fluxes and uncertainty at Bartlett Experimental Forest, NH (2004–2016).

	Components of Net Primary Production	Flux (g C/m <sup>2</sup> /yr)	95% confid	Biometric Method
(a)	Aboveground Wood (1 + 2 + 3)	204	29	
	1) Large trees (> 12.7 cm dbh)	143	20	Allometry using successive measures of DBH
	2) Small trees (< 12.7 cm dbh)	30	5	Allometry using successive measures of DBH
	3) branchfall	31	21	Annual branchfall tarps
(b)	Foliage, fruit, flower	123	11	Annual litterfall collection
(c)	Understory/herbivory	20	10	Allometry on microplots
(d)	Woody roots	34	7	Allometry using successive measures of DBH
(e)	Fine roots	110	64	Root ingrowth cores
(f)	Mycorrhizae	124	93	Stable isotope approach
(h)	NPP	615	118	(a + b + c + d + e + f)
	<b>Respiratory Fluxes</b>			
(i)	Total Soil Respiration	810	48	Manual and auto-chambers
(j)	CWD respiration	5	5	mass estimates of CWD and decay class specific loss rates
(k)	Standing dead respiration	56	15	allometry and decay class specific loss rates
(l)	Woody autotrophic respiration	153	114	0.118 of GPPB (derived from Litton et al., 2007 database)
(m)	Foliar respiration	149	20	leaf level measurements
(n)	Heterotrophic Soil Respiration	434	101	$1.92 + 0.534 * (i)$ ; derived from soil respiration database
(o)	Autotrophic Soil respiration	376	101	1 - (n)
	NEPEC	132	49	eddy covariance flux tower (-NEE)
	NEPB	120	156	(h - j - k - n)
	ΔC	133	34	modified inventory approach
	Re	1153	69	eddy covariance flux tower
	ReB	1172	127	(i + j + k + l + m)
	GPP	1285	62	eddy covariance flux tower
	GPPB	1292	194	(h + l + m + o)
	TBCA	656	54	(i - b - iii)



**Fig. 2.** Plot of the percent of available nighttime data during the growing season (circles) and mean annual ecosystem respiration (triangles) with changes in ustar, highlighting the tradeoff between data quantity and data quality at BEF.

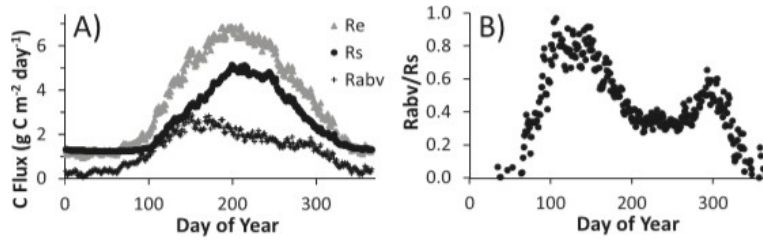


**Fig. 3.** A) Mean daily CO<sub>2</sub> flux by day of year for ecosystem respiration ( $Re_{EC}$ ), soil respiration ( $R_s$ ), and respiration from aboveground components of the ecosystem ( $R_{abv}$ ); B) Ratio of  $R_{abv}$  to  $R_s$  by day of year.

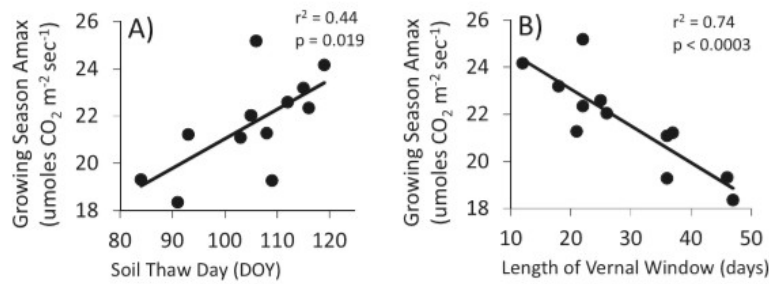


**Fig. 4.** Relationship between growing season canopy level  $A_{max}$  and (A) soil thaw day, and (B) the length of the vernal window during 2004–2016. The vernal window is defined as the number of days between soil thaw and the start of canopy gross carbon uptake.

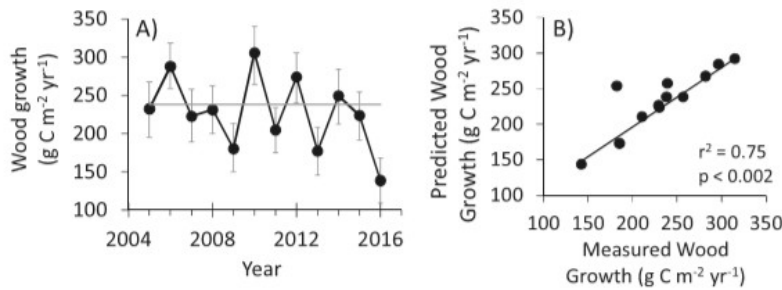


**Fig. 5.** A) Annual wood growth during 2004–2016 including both aboveground biomass and coarse roots. B) Predicted vs. measured wood growth. Predicted wood growth was estimated from a 2 parameter linear regression model using early summer air temperature (Julian days 136–215) and a drought index (the number of growing season days with VWC < 17.5%; 50% of the growing season mean VWC). The outlier in B) is 2013 where measured wood growth was much lower than predicted.